Synthesis and Mesogenic Properties of Rodlike Bis(alkylphenylazo)-Substituted *N,N′*-Salicylidenediaminato Nickel(II), Copper(II), and Oxovanadium(IV) Complexes

Iolinda Aiello, Mauro Ghedini,* Francesco Neve, and Daniela Pucci

Dipartimento di Chimica, Università della Calabria, I-87030 Arcavacata di Rende (CS), Italy

Received March 27, 1997. Revised Manuscript Received June 23, 1997[⊗]

The tetradentate Schiff base ligands *N,N′*-bis[5-(4′-*n*-alkyl)phenylazosalicylidene]alkyldiamine $H_2L_N(n)$ ($n = 6$, 14), based on 1,2-diaminoethane ($N = 1$), 1,3-diaminopropane ($N = 2$), and 1,3-diamino-2,2-dimethylpropane ($N = 3$) were prepared and characterized. For all the ligands complexes $M[L_N(n)]$ (M = Cu, Ni, VO) were readily obtained, which contained two free azo functions. The three series of complexes $M[L_N(n)]$ ($N = 1-3$) were investigated for mesomorphism. This was observed only for $N = 1$ or 2, in the form of enantiotropic nematic (lower homologues) or smectic (higher homologues) mesophases. The thermal behavior of complexes is discussed on the basis of the structural characteristics of the N,N chelate rings.

Introduction

Metallomesogens are metal-containing liquid-crystalline compounds whose different molecular structures and properties have been extensively reviewed.[1] These species are promising materials as a consequence of their electrical and optical features, and as such they are suitable for practical applications.[1c,h] Nevertheless, novel molecules with enhanced performance are still required. In this field we are concerned with the synthesis of either organometallic[2] or coordination compounds,[3] and we are currently focusing our attention on thermotropic metallomesogens bearing functional groups which can be relevant for electrooptical devices.

The development of mesomorphic materials for optical switching has recently emphasized the role of photoisomerizing species which exhibit a reversible isothermal phase transition. Azo-based mesogens[4−6] belong to this class of materials, since the trans−cis isomerization which takes place upon photoirradiation, reversibly converts the molecular shape from linear (trans −N=N−) to bent (cis −N=N−).[7] On the other hand, thermotropic 4,4′-disubstituted azobenzenes have been largely used as ligands to obtain cyclometalated palladium[8,9] or mercury[10] mesogens. In such a species the azo group is part of a five membered metallocycle, thus the trans ⇌ cis isomerization is prevented. Accordingly, to prepare rodlike liquid-crystalline compounds possessing both a metal center and the photoinduced capability to change molecular shape, new azobenzenes with a metal-bonding site other than $-C_6H_4-N=N-$ have to be designed.

The known metallomesogens which exhibit the uncomplexed −N=N− function are bowlic WO(VI) azo-substituted calix[4]arene derivatives[11] and calamitic Cu(II) complexes of {1-[4′-(4″-hexyloxyphenylazo)phenyl]-3-alkylamino-2-en-1-ones}.[12] With reference to the molecular shape we are interested in, we have designed the ligands shown in Scheme 1 (thereafter $H_2L_N(n)$) since they are expected to form metal complexes with ease.

Although our synthetic strategy takes advantage of previous studies showing that the bis(salicylaldheyde)-ethylenediimine (salen) is a suitable core for the synthesis of metallomesogens,[13−16] other structural elements have been also considered. In particular, with reference to the selected molecular fragments, while two aliphatic chains ($n = 6$ or 14) are essential to create an elongated structure, different diamines (namely 1,2-

* E-mail: ghedini@ccusc1.unical.it. Fax: (+39) 984 492062/492044.

[⊗] Abstract published in *Advance ACS Abstracts,* August 1, 1997.

(1) (a) Giroud-Godquin, A. M.; Maitlis, P. M. *Angew. Chem., Int. Ed. Engl.* **1991**, *30*, 375. (b) Espinet, P.; Esteruelas, M. A.; Oro, L. A.; Serrano, J. L.; Sola. E. *Coord. Chem. Rev.* **1992**, *117*, 215. (c) Bruce, D. W. In *Inorganic Materials*; Bruce, D. W.; O'Hare, D., Eds.; Wiley: Chichester, 1992. (d) Hudson, S. A.; Maitlis , P. M. *Chem. Rev.* **1993**, *93*, 861. (e) Polishchuk, A. E.; Timofeeva, T. V. *Russ. Chem. Rev.* **1993**, *62*, 291. (f) Oriol, L.; Serrano, J. L. *Adv. Mater.* **1995**, *7*, 348. (g) Deschenaux, R.; Goobdy, J. W. In *Ferrocenes*; Togni , A.; Hayashi, T., Eds.; VCH: Weinheim, 1995. (h) *Metallomesogens*; Serrano, J. L., Ed.; VCH: Weinheim, 1996. (i) Neve, F. *Adv. Mater.* **1996**, *8*, 277.

(2) (a) Ghedini, M.; Pucci, D.; Neve, F. *Chem. Commun.* **1996** 137. (b) Neve, F.; Ghedini, M.; Crispini, A. *Chem. Commun.* **1996**, 2463.

(3) (a) Ghedini, M.; Morrone, S.; Francescangeli, O.; Bartolino, R. *Mol. Cryst. Liq. Cryst.* **1994**, *250*, 323. (b) Neve, F.; Ghedini, M.; Francescangeli, O. *Liq. Cryst.* **1996**, *21*, 625.

(4) Xie, S., Natansohn, A.; Rochon, P. *Chem. Mater.* **1993**, *5*, 403.

(5) Ikeda, T.; Tsutsumi, O. *Science* **1995**, *268*, 1873.

(6) Newton, J.; Walton, H.; Coles, H.; Hodge, P. *Mol. Cryst. Liq. Cryst.* **1995**, *260*, 107.

(7) Rau, H. In *Photochromism*; Dürr, H. Ed.; Elsevier: Amsterdam, 1990.

(8) Hoshino, N.; Hasegawa, H.; Matsunaga, Y. *Liq. Cryst.* **1991**, *9*, 267.

(9) Crispini, A.; Ghedini, M.; Morrone, S., Pucci, D.; Francescangeli, O. *Liq. Cryst.* **1996**, *20*, 67 and references therein.

(10) Omenat, A.; Ghedini, M. *J. Chem. Soc., Chem. Commun.* **1994**, 1309.

(11) Xu, B.; Swager, T. M. *J. Am. Chem. Soc.* **1993**, *115*, 1159.

(12) Szydlowska, J.; Pyzuk, W., Krowczynsky, A.; Bikchantaev, I. *J. Mater. Chem.* **1996**, *6*, 733.

(13) (a) Paschke, R.; Zaschke, H.; Madicke, A.; Chipperfield, J. R.; Blake, A. B.; Nelson, P. G.; Gray, G. W. *Mol. Cryst. Liq. Cryst. Lett.* **1988**, *6*, 81. (b) Paschke, R.; Balkow, D.; Baumeister, U.; Hartung, H.; Chipperfield, J. R.; Blake, A. B.; Nelson, P. G.; Gray, G. W. *Mol. Cryst. Liq. Cryst.* **1990**, *188*, 105. (c) Blake, A. B.; Chipperfield, J. R.; Hussain, W.; Paschke, R.; Sinn, E. *Inorg. Chem.* **1995**, *34*, 1125.

(14) (a) Shaffer, T. D.; Sheth, K. A. *Mol. Cryst. Liq. Cryst.* **1989**, *172*, 27. (b) Ohta, K.; Morizumi, Y.; Fujimoto, T.; Yamamoto, I.; Miyamura, K.; Gohshi, Y. *Mol. Cryst. Liq. Cryst.* **1992**, *214*, 161.

(15) Moore, J. S.; Stupp, S. I. *Polym. Bull.* **1988**, *19*, 251.

(16) Serrette, A.; Carrol, P. J.; Swager, T. M. *J. Am. Chem. Soc.* **1992**, *114*, 1887.

S0897-4756(97)00176-2 CCC: $14.00

Scheme 1

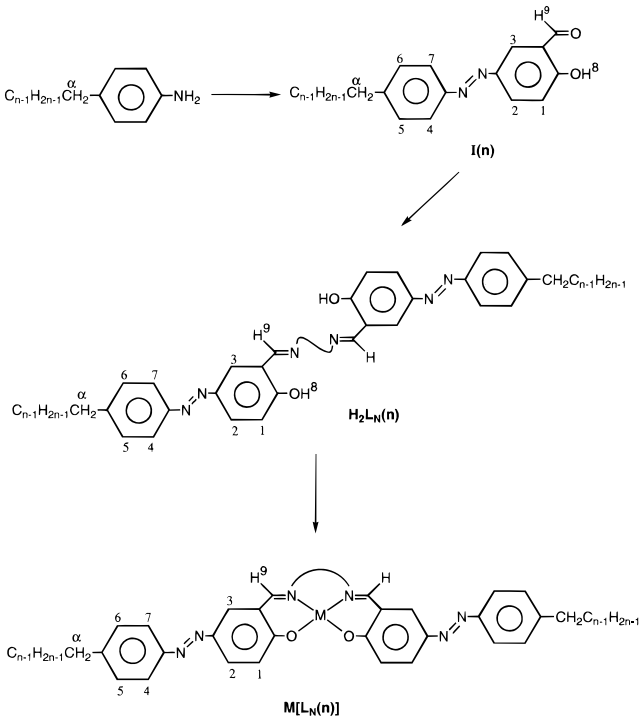

diaminoethane, $N = 1$; 1,3- diaminopropane, $N = 2$; 1,3-diamino-2,2-dimethylpropane, $N = 3$) have been used to test the role of the metal environment in promoting mesomorphism.[16] In this paper we describe the synthesis and thermotropic behavior of both $H_2L_N(n)$ ligands and M[$L_2(n)$] complexes (M = Ni, Cu, VO).

Results

Syntheses. The preparation of the $H_2L_N(n)$ compounds (Scheme 1) was accomplished by condensation of the selected diamines with the 2-hydroxy-5-(4′-*n*-alkyl)phenylazobenzaldehydes **I**(*n*), which in turn result from coupling of the appropriate diazonium chloride with salicylaldehyde. $H_2L_N(n)$ ligands are yellow-orange solids (yields, melting points, analytical data and ^{1}H NMR spectra in the Experimental Section) that afford the respective metal derivatives by reaction with M(II) (M = Cu, Ni) or VO(IV) salts.

The M[$L_N(n)$] complexes, solids whose color depends on the nature of the metal center, were characterized by elemental analysis, IR and, in the case of the diamagnetic Ni(II) species, ^{1}H NMR spectroscopies (Experimental Section). The bonding mode of the $L_N(n)$ ligands for the Ni complexes has been inferred by ^{1}H NMR evidence. This shows that the Ni(II) ion selectively binds the *O*,*N*,*N*,*O*-tetradentate salen-type functionality. Strong indications of Ni binding arise from both the large shielding experienced by the imine proton H^9 ($\Delta\delta = \delta_{ligand} - \delta_{complex} = 0.9-1.2$ ppm) and the disappearance of the proton signal corresponding to the OH group of the free ligands. Infrared data are much less informative[17] (C=N and N=N stretching modes superimpose in the same region), although they are not in contrast with the presence of tetradentate ligands with an N_2O_2 donor set. By analogy, a similar bonding mode has been proposed for the homologous paramagnetic Cu(II) and VO(IV) compounds (Scheme 1).

The metal coordination geometry cannot be reliably predicted along the whole series. Whereas Ni(II) complexes are usually square planar[13b,c] and Cu(II) species are probably similar,[13,14a] VO(IV) complexes with salen-type ligands can give rise either to monomeric structures[18,19] with square-pyramidal coordination geometry or to polymeric structures[16,19,20] with {V=O···V=O···} interactions which afford a distorted octahedral coordination. However, it has been reported that, in the absence of X-ray crystal structures, the monomeric or polymeric nature of these compounds can be assigned on the basis of IR spectra,[16,18−21] which show ν(V=O) at about 980 cm^{-1} for the monomers and nearly at 880 cm^{-1} for the polymers. In the present case, the VO[$L_1(n)$] compounds exhibit a ν(V=O) at about 988 cm^{-1}, whereas in the remaining VO[$L_2(n)$] and VO[$L_3(n)$] complexes, ν(V=O) appears around 870 cm^{-1}. Consequently, a square-pyramidal coordination is assigned to the salen derivatives ($N = 1$ in Scheme 1) and an octahedral coordination to both the 1,3-diaminopropane and 1,3-diamino-2,2-dimethylpropane derivatives ($N = 2$ and 3 in Scheme 1, respectively).

Mesomorphism. None of the $H_2L_N(n)$ ligands displays thermotropic mesomorphism and upon heating they all melt at temperatures which progressively decrease with either increasing the bridge size ($N = 1-3$) or the alkyl chain length ($n = 6$ to $n = 14$). Thus, the melting points of the whole $H_2L_N(n)$ series ranges from 211 °C for $H_2L_1(6)$ to 120 °C for $H_2L_3(14)$.

Mesophases always form upon metal complexation except for the $H_2L_3(n)$ derivatives. The different mesophases were recognized through optical observations. In some cases, an unambigous assignment was difficult to gain because of the dark colors of the textures and for the high temperature at which the phase transitions occur. Moreover, approaching the transition to the isotropic liquid phase a considerable amount of decomposition was detected for all the complexes (exothermic peaks in the DSC trace). Hence, variable-temperature low-angle X-ray diffraction (XRD) investigations were performed only on the mesogens featuring the comparatively higher thermal stability (with respect to decomposition) and lower melting points. The phase behavior (namely transition temperatures, phase assignments and enthalpy changes) for the M[$L_N(n)$] complexes ($N = 1$, 2) is shown in Table 1.

The $H_2L_1(n)$ and $H_2L_2(n)$ series give rise to Ni(II)-, Cu(II)-, or VO(IV)-containing polymorphic materials which display enantiotropic smectic C (S_C) or nematic (N) mesomorphism (Table 1). A typical schlieren texture (Figure 1) was observed in both N and Sc phases. In some cases, the schlieren texture the Sc phase took a blurred appearance.[22] For all complexes a pseudo-isotropic texture or an oily streak texture was observed

(17) (a) Holm, R. H.; Everett, G. W.; Chakavorty, A. *Prog. Inorg. Chem.* **1966**, *7*, 83. (b) Calligaris, M.; Randaccio, L. In *Comprehensive Coordination Chemistry*; Wilkinson, G., Gillard, R., McCleverty, J. A., Eds.; Pergamon Press: Oxford, UK, 1987; Vol. 2, Chapter 20.1.

(18) Riley, P. E.; Pecoraro, V. L.; Carrano, C. J.; Bonadies, J. A.; Raymond, K. N. *Inorg. Chem.* **1986**, *25*, 154.

(19) (a) Kasahara, R.; Tsuchimoto, M.; Ohba, S.; Nakajima, K.; Ishida, H.; Kojima, M. *Inorg. Chem.* **1996**, *35*, 7661. (b) Nakajima, K.; Kojima, M.; Azuma, S.; Kasahara, R.; Tsuchimoto, M.; Kubozono, Y.; Maeda, H.; Kashino, S.; Ohba, S.; Yoshikawa, Y.; Fujita, *J. Bull. Chem. Soc. Jpn.* **1996**, *69*, 3207.

(20) Mathew, M.; Carty, A. J.; Palenik, G. J. *J. Am. Chem. Soc.* **1970**, *92*, 3197.

(21) Hamilton, D. E. *Inorg. Chem.* **1991**, *30*, 1670.

Table 1. Transition Temperatures, Phase Assignments, and Enthalpy Changes for the M[$L_N(n)$] Complexes (N = 1, 2)

compound	transition	T/°C [a]	ΔH/kJ mol^{-1}
Ni[L_1(6)]	C−N	287.6	14.97
	N−I_{dec}	307.9	
Cu[L_1(6)]	C−N	290.1	16.20
	N−I_{dec}	313.6	
VO[L_1(6)]	C−C′	252.8	3.48
	C′−S	304.9	7.89
	S−I_{dec}	320.4	
Ni[L_1(14)]	C−Sc	262.6	13.44
	Sc−I_{dec}	312.0	
Cu[L_1(14)]	C−Sc	285.8	15.46
	Sc−I_{dec}	310.4	
VO[L_1(14)]	C−C′	266.4	1.09
	C′−Sc	271.1	21.89
	Sc−I_{dec}	328.6	
Ni[L_2(6)]	C−N	223.1	10.53
	N−I_{dec}	257.2	
Cu[L_2(6)]	C−N	240.3	9.69
	N−I_{dec}	301.5	
VO[L_2(6)]	C−I_{dec}	380.0 [b]	
Ni[L_2(14)]	C−Sc	173.4	8.17
	Sc−I_{dec}	302.2	
Cu[L_2(14)]	C−Sc	190.7	9.16
	Sc−I_{dec}	300.4	
VO[L_2(14)]	C−C′	266.4	1.11
	C′−Sc	271.1	22.23
	Sc−I_{dec}	328.6	

[a] C, crystal; S, smectic; N, nematic; I, isotropic liquid; dec, decomposition. [b] From optical microscopy.

on submitting the sample to mechanical stress (light compression or shearing force). The appearance of some textural characteristics peculiar to twisted phases is rather unexplained, although we cannot exclude that a certain degree of twisting could occur by surface interaction. However, as already stated the high tendency of these mesogens to undergo decomposition makes more difficult the interpretation of textural features.

The Sc mesophase of Ni[L_2(14)] and Cu[L_2(14)] was confirmed by the XRD spectra which revealed only one sharp peak at low angle. The corresponding layer thicknesses were found to be 49.4 Å (at 190 °C) for the Ni(II) complex and 47.7 Å (at 195 °C) for the Cu(II) one. Taking into account that the molecular length of the compounds calculated in the most extended conformation is ca. 56 Å, the tilt angle for Ni[L_2(14)] and Cu[L_2(14)] is 28 and 32°, respectively. In both cases, it was also noted that the tilt angle varies only slightly with temperature (at least up to the upper limit—ca. 220 °C—of the experimental setup).

For the sake of comparison, the phase transition temperatures for M[$L_N(n)$] (N = 1, 2) are plotted for the different metal ions in Figure 2. For Ni(II) and Cu(II) complexes the length of the terminal alkyl chains influences the type of mesophase, and the usual trend is observed. Thus, a short chain (n = 6) induces a nematic phase while a longer one (n = 14) causes a more ordered mesophase (S_C) to appear. VO(IV) mesogens behave differently, as a S_C phase is observed whatever the number of carbon atoms in the alkyl chain. In one case (VO[L_2(6)]) no mesomorphism was seen. However, these thermotropic species show that, with a few exceptions, the melting temperature decreases and the thermal stability increases with increasing n.

(22) Demus, D.; Richter, L. *Textures of liquid crystals*; Verlag Chemie: Weinheim, Germany, 1978; p 82.

Discussion

The $H_2L_N(n)$ molecules, despite the two mesogenic alkylphenylazo fragments they contain, do not give liquid-crystalline materials. A possible explanation for this behavior may be from the transoid N,N conformation which stabilizes a stepped molecular geometry (Scheme 1) that discourage mesomorphism. Unfortunately, in support of such a statement only few data are available from the literature. Nevertheless, comparing these $H_2L_N(n)$ ligands with the similar bis(alkyloxy)-*N*,*N*′-salicylidenediamines it can be seen that while compounds **I** (Scheme 2) are not mesomorphic,[13c] compounds **II** (Scheme 2) are.[23]

Metal complexation of the $H_2L_N(n)$ (N = 1, 2) species induces mesomorphism. According to the above discussion concerning the geometry suggested for the uncomplexed ligands, this result can be ascribed to the rodlike molecular shape which the complexes adopt (Scheme 1).

With reference to the *N*,*N*-chelating ring, both the 1,2-diaminoethane and 1,3-diaminopropane derivatives, M[$L_1(n)$] and M[$L_2(n)$], respectively, exhibit liquid crystallinity (Table 1). In addition, comparing these species, it is worth noting that the M[$L_2(n)$] complexes display mesophases which are stable over considerably wider temperature ranges and appear at lower temperatures (Table 1 and Figure 2). Thus, the present data show the mesogenic aptitude of both the N−$(CH_2)_2$−N (N = 1) and N−$(CH_2)_3$−N (N = 2) bridges and point out that changing the N−$(CH_2)_3$−N bridge (N = 2) for N−CH_2−$C(Me)_2CH_2$−N (N = 3), the liquid-crystalline properties are suppressed.

The mesogenic properties of the whole M[$L_N(n)$] series can be conveniently discussed taking into account the structural features of the N,N-chelate ring. The five-membered ring (N = 1) is roughly planar while the six-membered ones (N = 2, 3) take a chair form which displaces out of the O,N,N,O plane the −CH_2− (N = 2) or the bulkier −$C(Me)_2$− (N = 3) groups.[18] Thus, the *N*,*N*-chelate ring is expected to help the molecular packing as follows: N−$(CH_2)_2$−N (N = 1) > N−$(CH_2)_3$−N (N = 2) > N−CH_2−$C(Me)_2CH_2$−N (N = 3). Indeed this trend parallels the observed mesomorphism (e.g., melting temperatures lower for M[$L_2(n)$] than for M[$L_1(n)$]) and suggests that the absence of mesomorphism for M[$L_3(n)$] can be attributed to the bulkiness of the −$C(Me)_2$− group.

Mesogens containing the RO- or R-substituted salen core and incorporating Ni(II),[13,14] Cu(II),[13,14a] or VO(IV)[16] were previously reported. Interestingly, none of these compounds display the nematic phase shown by the complexes Ni[L_N(6)] and Cu[L_N(6)] (N = 1, 2).

The thermotropic behavior of compounds with a metal atom coordinated as in M[$L_2(n)$] or in M[$L_3(n)$] was previously investigated for VO(IV).[16] The molecular structures of these species differ from those of VO[$L_N(n)$] as two alkoxy chains replace the two R−C_6H_4−N=N− fragments. Solid VO[$L_N(n)$] (N = 2, 3) contain the polymeric {V=O···V=O···} array thus the liquid-crystalline state should be brought about by the appropriate balance between the effect exerted by the azo-substituents and the puckering of the VO environment. Indeed mesomorphism appears for an isolated VO center placed in a rigid environment (N = 1) or for

(23) Ghedini, M.; Aiello, I., unpublished results.

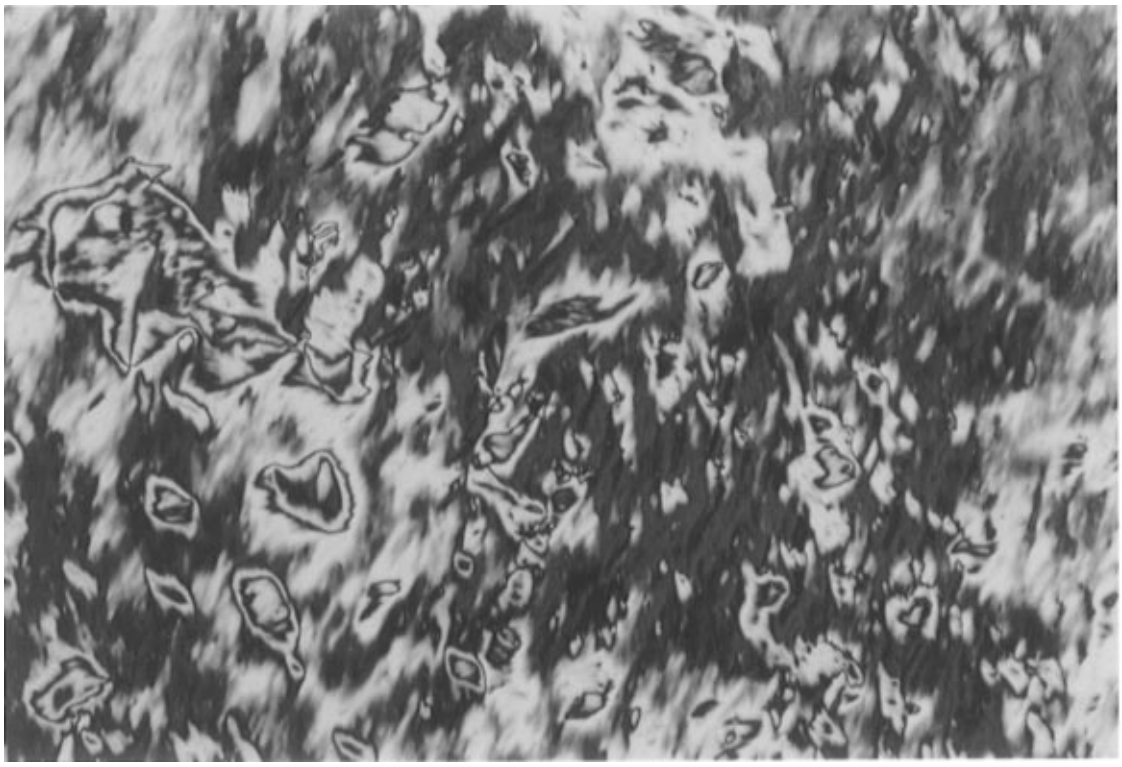

Figure 1. Schlieren texture shown by the Sc phase of **Cu[L_2(14)]** at 215 °C.

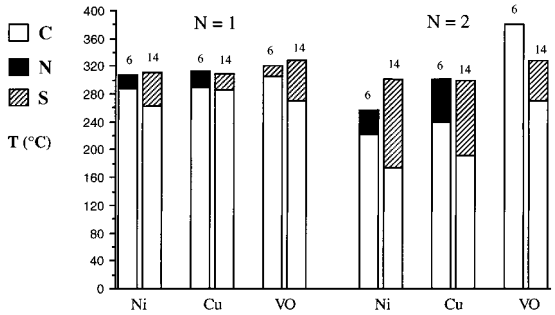

Figure 2. Mesomorphic behavior of the **M[L_N(*n*)]** complexes (M = Ni, Cu, VO; N = 1, 2; *n* = 6, 14.)

{V═O···V═O···} systems wherein VO is part of a non planar chelate ring (*N* = 2). In the presence of V═O···V═O contacts, the mesomophism is lost in molecular structures bearing a more sterically hindered *N*,*N*-chelate ring (*N* = 3). By contrast, this latter destabilizing effect has also been invoked to explain the appearance of mesomorphism when the R−C_6H_4−N═N− group is changed for an alkoxy one.[16] The above observations call for a relevant role played by the alkylphenylazo substituents in determining the mesomorphism of these species. At this stage this role seems to be a conflicting one, as it is promoting (*N* = 1, 2) or suppressing (*N* = 3) at the same time.

In conclusion, the synthesis of some representative examples of both smectic and nematic metallomesogens containing the free −N═N− group has been successfully achieved. Their clearing temperatures depend on the nature of the metal ion and along homologous series decrease according to the following trend VO(IV) > Cu(II) ≈ Ni(II). Notably, the M[L_2(14)] series displays the widest mesomorphic ranges. Therefore, provided the isotropization temperatures (where decomposition occurs) are not reached, these smectic compounds and the nematic M[L_2(6)] (M = Ni, Cu) as well, are suitable materials for further investigation concerning possible applications.

Scheme 2

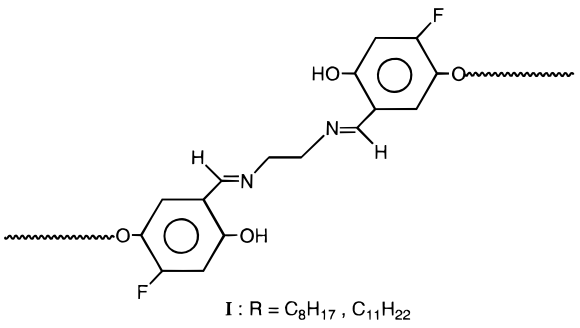

I : R = C_8H_{17} , $C_{11}H_{22}$

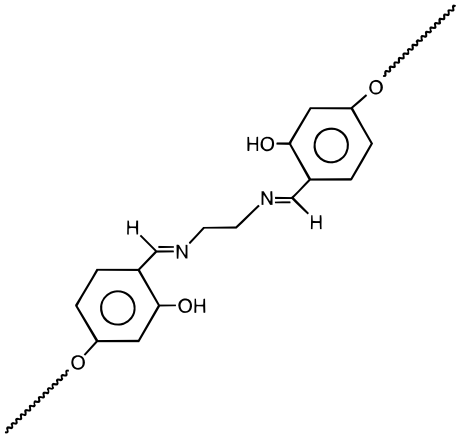

II : R = $C_{10}H_{21}$, $C_{12}H_{25}$, $C_{14}H_{29}$, $C_{18}H_{37}$

Experimental Section

General Procedure. The infrared spectra were recorded on a Perkin-Elmer F.T.2000, as KBr pellets. The ^{1}H NMR spectra were recorded on a Bruker WH-300 spectrometer in $CDCl_3$ solutions, with TMS as internal standard. Elemental analyses were performed with a Perkin-Elmer 2400 analyzer.

The optical observations were made with a Zeiss Axioscope polarizing microscope equipped with a Linkam C0 600 heating stage. The transition temperatures and enthalpies were measured on a Perkin-Elmer DSC-7 differential scanning calorimeter with a heating and cooling rate of 10.0 °C/min. The apparatus was calibrated with indium (156.6 °C, 3.3 kJ mol^{-1}) and tin (232.1 °C, 7.2 kJ mol^{-1}). The X-ray diffraction measurements were performed with a INEL CPS-120 powder diffractometer using a monochromatized Cu Kα radiation (λ = 1.54 Å).

All the commercially available chemicals were used without further purification.

Synthesis of the Ligands. *Preparation of 2-Hydroxy-5-(4′-n-alkyl)phenylazobenzaldehyde,* ***I(n)***. In a typical preparation, 15 mL of H_2O containing HCl (1.41 mL, 12 M, 16.92 mmol) were added to the appropriate 4-alkyl-substituted aniline (1.00 g, 5.64 mmol). To the resulting solution, stirred and cooled to 0 °C, an aqueous $NaNO_2$ (0.42 g, 6.09 mmol) solution (6 mL) was added dropwise, and the so-formed diazonium chloride was consecutively coupled with salicylaldehyde (0.69 g, 5.64 mmol), dissolved in 6.5 mL of aqueous 2N NaOH (0.52 g, 12.97 mmol) solution. The reaction mixture was stirred for 1 h at 0 °C and then allowed to warm slowly to room temperature. The brown precipitate which formed was filtered, washed several times with H_2O, dissolved in CH_2Cl_2 and the resulting solution dried over anhydrous Na_2SO_4. The crude product **I(*n*)**, obtained after removal of the solvent under reduced pressure, was purified by column chromatography (SiO_2, diethyl ether/hexane, 1/9 v/v).

Colors, yields, melting points, NMR data, and elemental analyses are as follows.

2-hydroxy-5-(4′-n-hexyl)phenylazobenzaldehyde, ***I(6)***. Yellow. Yield 52%. Mp 108 °C. ^{1}H NMR (300 MHz, $CDCl_3$) δ 11.30 (s, H^8), 10.03 (s, H^9), 8.14 (d, H^2), 8.17 (s, H^3), 7.82 (d, $H^{4,7}$), 7.32 (d, $H^{5,6}$), 7.11 (d, H^1), 2.69 (t, H^α). Anal. Calcd for $C_{19}H_{22}N_2O_2$: C, 73.52; H, 7.14; N, 9.02. Found: C, 73.72; H, 7.08; N, 9.34.

2-hydroxy-5-(4′-n-tetradecyl)phenylazo-benzaldehyde, ***I(14)***. Yellow. Yield 60%. Mp 104 °C. ^{1}H NMR (300 MHz, $CDCl_3$) δ 11.30 (s, H^8), 10.03 (s, H^9), 8.15 (d, H^2), 8.18 (s, H^3), 7.82 (d, $H^{4,7}$), 7.32 (d, $H^{5,6}$), 7.11 (d, H^1), 2.69 (t, H^α). Anal. Calcd for $C_{27}H_{38}N_2O_2$: C, 76.74; H, 9.06; N, 6.63. Found: C, 76.75; H, 8.91; N, 6.65.

Preparation of N,N′-bis[-2-hydroxy-5-(4′-n-alkyl)phenylazobenzylidene]alkyldiamine, ***$H_2L_N(n)$***. **H_2L_1(6). I(6)** (300 mg, 0.97 mmol) and 1,2-diaminoethane (0.03 mL, 0.48 mmol) were mixed in ethanol (50 mL) and stirred under reflux for 4 h. The yellow-orange precipitate which immediately formed was filtered, washed with cold ethanol, and vacuum-dried. Yield 92%. Mp 211 °C. ^{1}H NMR (300 MHz, $CDCl_3$) δ 13.71 (s, H^8), 8.49 (s, H^9), 7.95 (dd, H^2), 7.88 (d, H^3), 7.78 (d, $H^{4,7}$), 7.29 (d, $H^{5,6}$), 7.05 (d, H^1), 2.67 (t, H^α), 4.01 (s, =N−CH_2). Anal. Calcd for $C_{40}H_{48}N_6O_2$: C, 74.50; H, 7.50; N, 13.03. Found: C, 74.47; H, 7.40; N, 13.46.

All the analogous **$H_2L_N(n)$** compounds were prepared as described for **H_2L_1(6)**. Colors, yields, melting points, NMR data and elemental analyses are as follows:

H_2L_1(14). Yellow-orange. Yield 93%. Mp 186 °C. ^{1}H NMR (300 MHz, $CDCl_3$) δ 13.72 (s, H^8), 8.50 (s, H^9), 7.94 (dd, H^2), 7.89 (d, H^3), 7.78 (d, $H^{4,7}$), 7.29 (d, $H^{5,6}$), 7.05 (d, H^1), 2.67 (t, H^α), 4.02 (s, =N−CH_2). Anal. Calcd for $C_{56}H_{80}N_6O_2$: C, 77.37; H, 9.27; N, 9.66. Found: C, 77.76; H, 9.27; N, 10.15.

H_2L_2(6). Yellow-orange. Yield 87%. Mp 148 °C. ^{1}H NMR (300 MHz, $CDCl_3$) δ 14.05 (s, H^8), 8.49 (s, H^9), 7.97 (dd, H^2), 7.89 (d, H^3), 7.78 (d, $H^{4,7}$), 7.29 (d, $H^{5,6}$), 7.06 (d, H^1), 2.66 (t, H^α), 3.78 (t, =N−CH_2), 2.18 (m, −CH_2). Anal. Calcd for $C_{41}H_{50}N_6O_2$: C, 74.74; H, 7.65; N, 12.75. Found: C, 74.21; H, 7.67; N, 12.27.

H_2L_2(14). Yellow-orange. Yield 86%. Mp 133 °C. ^{1}H NMR (300 MHz, $CDCl_3$) δ 14.00 (s, H^8), 8.50 (s, H^9), 7.97 (dd, H^2), 7.89 (d, H^3), 7.78 (d, $H^{4,7}$), 7.29 (d, $H^{5,6}$), 7.07 (d, H^1), 2.66 (t, H^α), 3.79 (t, =N−CH_2), 2.19 (m, −CH_2). Anal. Calcd for $C_{57}H_{82}N_6O_2$: C, 77.51; H, 9.36; N, 9.51. Found: C, 77.58; H, 9.40; N, 9.43.

H_2L_3(6). Yellow-orange. Yield 90%. Mp 134 °C. ^{1}H NMR (300 MHz, $CDCl_3$) δ 14.17 (s, H^8), 8.46 (s, H^9), 7.98 (dd, H^2), 7.91 (d, H^3), 7.79 (d, $H^{4,7}$), 7.29 (d, $H^{5,6}$), 7.08 (d, H^1), 2.66 (t, H^α), 3.56 (s, =N−CH_2), 1.12 (s, −CH_3). Anal. Calcd for $C_{43}H_{54}N_6O_2$: C, 75.18; H, 7.92; N, 12.90. Found: C, 75.52; H, 7.97; N, 12.09.

H_2L_3(14). Yellow-orange. Yield 82%. Mp 120 °C. ^{1}H NMR (300 MHz, $CDCl_3$) δ 14.13 (s, H^8), 8.46 (s, H^9), 7.98 (dd, H^2), 7.91 (d, H^3), 7.78 (d, $H^{4,7}$), 7.29 (d, $H^{5,6}$), 7.07 (d, H^1), 2.66 (t, H^α), 3.56 (s, =N−CH_2), 1.12 (s, −CH_3). Anal. Calcd for $C_{59}H_{86}N_6O_2$: C, 77.76; H, 9.52; N, 9.22. Found: C, 77.20; H, 9.30; N, 8.99.

Synthesis of the Metal Complexes M[$L_N(n)$]. *Preparation of* ***Ni[L_1(6)]***. KOH (17 mg, 0.31 mmol) and nickel(II) acetate tetrahydratate (38.0 mg, 0.15 mmol) were added to a stirred suspension of **H_2L_1(6)** (100 mg, 0.15 mmol) in ethanol (15 mL) heated to reflux. An ochre precipitate immediately formed which was stirred under reflux for 2 h, then cooled to room temperature, filtered, and crystallized from chloroform-ethanol. Yield 85%. ^{1}H NMR (300 MHz, $CDCl_3$) δ 7.92 (dd, H^2), 7.72 (d, $H^{4,7}$), 7.70 (br s, H^3), 7.58 (s, H^9), 7.23 (d, $H^{5,6}$), 7.10 (d, H^1), 2.65 (t, H^α), 3.54 (s, =N−CH_2). Anal. Calcd for $C_{40}H_{46}N_6O_2Ni$: C, 68.48; H, 6.61; N, 11.98. Found: C, 68.96; H, 6.70; N, 12.93. The thermal behavior is reported in Table 1.

The homologous **M[$L_N(n)$]** complexes were synthesized following the procedure described for **Ni[L_1(6)]** reacting the pertinent ligands with copper acetate dihydrate or vanadyl acetate. Their thermal behavior are reported in Table 1 while colors, yields, melting points, NMR and IR data and elemental analyses are as follows.

Ni[L_1(14)]. Ochre. Yield 88%. ^{1}H NMR (300 MHz, $CDCl_3$) δ 7.94 (dd, H^2), 7.72 (d, $H^{4,7}$), 7.70 (br s, H^3), 7.58 (s, H^9), 7.26 (d, $H^{5,6}$), 7.10 (d, H^1), 2.65 (t, H^α), 3.54 (s, =N−CH_2). Anal. Calcd for $C_{56}H_{78}N_6O_2Ni$: C, 72.64; H, 8.49; N, 9.08. Found: C, 71.91; H, 8.44; N, 9.00.

Ni[L_2(6)]. Brownish green. Yield 83%. ^{1}H NMR (300 MHz, $CDCl_3$) δ 7.86 (dd, H^2), 7.70 (d, $H^{4,7}$), 7.63 (d, H^3), 7.29 (s, H^9), 7.22 (d, $H^{5,6}$), 7.03 (d, H^1), 2.67 (t, H^α), 3.55 (br t, =N−CH_2), 1.92 (m, −CH_2). Anal. Calcd for $C_{41}H_{48}N_6O_2Ni$: C, 68.82; H, 6.76; N, 11.74. Found: C, 67.85; H, 6.45; N, 11.55.

Ni[L_2(14)]. Ochre. Yield 80%. ^{1}H NMR (300 MHz, $CDCl_3$) δ 7.89 (d, H^2), 7.73 (d, $H^{4,7}$), 7.73 (d, H^3), 7.46 (s, H^9), 7.29 (d, $H^{5,6}$), 7.08 (d, H^1), 2.66 (t, H^α), 3.66 (t, =N−CH_2), 2.00 (m, −CH_2). Anal. Calcd for $C_{57}H_{80}N_6O_2Ni$: C, 72.83; H, 8.58; N, 8.94. Found: C, 71.94; H, 8.28; N, 8.73.

Ni[L_3(6)]. Brownish green. Yield 70%. Mp 295 °C. ^{1}H NMR (300 MHz, $CDCl_3$) δ 7.88 (dd, H^2), 7.72 (d, $H^{4,7}$), 7.69 (d, H^3), 7.24 (d, $H^{5,6}$ and H^9), 7.08 (d, H^1), 2.64 (t, H^α), 3.34 (s, =N−CH_2), 0.97 (s, −CH_3). Anal. Calcd for $C_{43}H_{52}N_6O_2Ni$: C, 69.45; H, 7.05; N, 11.3. Found: C, 69.66; H, 7.02; N, 11.5.

Ni[L_3(14)]. Ochre. Yield 57%. Mp 248 °C. ^{1}H NMR (300 MHz, $CDCl_3$) δ 7.89 (dd, H^2), 7.74 (d, $H^{4,7}$), 7.71 (d, H^3), 7.25 (d, $H^{5,6}$ and H^9), 7.10 (d, H^1), 2.65 (t, H^α), 3.34 (s, =N−CH_2), 0.98 (s, −CH_3). Anal. Calcd for $C_{59}H_{84}N_6O_2Ni$: C, 73.20; H, 8.75; N, 8.68. Found: C, 74.45; H, 8.76; N, 8.75.

Cu[L_1(6)]. Olive green. Yield 81%. Anal. Calcd for $C_{40}H_{46}N_6O_2Cu$: C, 68.01; H, 6.56; N, 11.90%. Found: C, 68.20; H, 6.75; N, 12.6.

Cu[L_1(14)]. Dark green. Yield 70%. Anal. Calcd for $C_{56}H_{80}N_6O_3Cu$: C, 70.89; H, 8.50; N, 8.86. Found: C, 71.02; H, 8.00; N, 9.23.

Cu[L_2(6)]. Dark green. Yield 87%. Anal. Calcd for $C_{41}H_{50}N_6O_3Cu$: C, 66.69; H, 6.82%; N, 11.38. Found: C, 67.27; H, 6.39; N, 12.06.

Cu[L_2(14)]. Brownish yellow. Yield 80%. Anal. Calcd for $C_{57}H_{82}N_6O_3Cu$: C, 71.10; H, 8.58; N, 8.73. Found: C, 71.13; H, 8.23; N, 9.14.

Cu[L_3(6)]. Dark green. Yield 85%. Mp 270 °C. Anal. Calcd for $C_{43}H_{52}N_6O_2Cu$: C, 69.00; H, 7.00; N, 11.23. Found: C, 68.51; H, 6.88; N, 10.94.

Cu[L_3(14)]. Olive green. Yield 85%. Mp 221 °C. Anal. Calcd for $C_{59}H_{84}N_6O_2Cu$: C, 72.84; H, 8.60% N, 8.82. Found: C, 72.44; H, 8.60; N, 8.82.

VO[L_1(6)]. Dark green. Yield 81%. ν(V═O) 988 cm^{-1}. Anal. Calcd for $C_{40}H_{46}N_6O_3V$: C, 67.68; H, 6.53; N, 11.84. Found: C, 68.21; H, 6.81; N, 11.79.

VO[L_1(14)]. Olive green. Yield 78%. ν(V═O) 988 cm^{-1}. Anal. Calcd for $C_{56}H_{78}N_6O_3V$: C, 72.00; H, 8.42; N, 9.00. Found: C, 71.19; H, 8.32; N, 9.08.

VO[L_2(6)]. Ochre. Yield 87%. ν(V═O) 873 cm^{-1}. Anal. Calcd for $C_{41}H_{48}N_6O_3V$: C, 68.04; H, 6.68; N, 11.61. Found: C, 67.96; H, 6.10; N, 11.90.

VO[L_2(14)]. Ochre. Yield 78%. ν(V═O) 862 cm^{-1}. Anal. Calcd for $C_{57}H_{80}N_6O_3V$: C, 72.20; H, 8.50; N, 8.86. Found: C, 71.12; H, 8.38; N, 8.85.

VO[L_3(6)]. Ochre. Yield 69%. Mp 353 °C. ν(V═O) 873 cm^{-1}. Anal. Calcd for $C_{43}H_{52}N_6O_3V$: C, 68.69; H, 6.97; N, 11.18. Found: C, 67.64; H, 6.53; N, 10.39.

VO[L_3(14)]. Ochre. Yield 74%. Mp 318 °C. ν(V═O) 874 cm^{-1}. Anal. Calcd for $C_{59}H_{84}N_6O_3V$: C, 72.59; H, 8.67; N, 8.61. Found: C, 71.64; H, 8.19; N, 8.58.

Acknowledgment. The present work was partially supported by the Italian Ministero dell'Università e della Ricerca Scientifica e Tecnologica (MURST) and Consiglio Nazionale delle Ricerche (CNR). We wish to thank Dr. Oriano Francescangeli (Università di Ancona) for the XRD measurements.

CM9701769